Timothy STEENHAUT,[a*] Yaroslav FILINCHUK[a*] and Sophie HERMANS[a*]
[a] Université catholique de Louvain, IMCN, Place Louis Pasteur 1, 1348 Louvain-la-Neuve, Belgium
[*] Address: Place Louis Pasteur 1, L.04.01.03, 1348 Louvain-la-Neuve, Belgium
timothy.steenhaut@uclouvain.be (orcid.org/0000-0003-2881-9440),
yaroslav.filinchuk@uclouvain.be (orcid.org/0000-0002-6146-3696),
sophie.hermans@uclouvain.be (orcid.org/0000-0003-4715-7964)

Synthesis strategies towards new heterometallic and functionalized metal-organic frameworks

Synthesis strategies towards new heterometallic and functionalized metal-organic frameworks

Abstract
Metal-organic frameworks (MOFs) are promising materials for many applications, including, but not limited to, gas sorption and storage, catalysis, drug delivery, removal of pollutants and sensing of chemicals. Although they are versatile materials, their synthesis is often associated with the use of toxic and sometimes dangerous chemicals, and usually require a significant energy for heating and pressurizing purposes, as most current methodologies involve solvothermal steps. Herein, we describe new and greener methodologies for the synthesis of three types of MOFs; namely MIL-100, MOF-76 and HKUST-1, possessing particularly interesting structures and potential applications, and their modification by addition of secondary metals or new functionalities to achieve materials imparted with new or improved properties. Those syntheses are achieved at low temperatures, in benign solvents such as water or ethanol, or through mechanochemistry. In addition, the impact of the synthesis parameters on the obtained materials was studied, as well as the possibility to further post-functionalize the obtained structures. The obtained materials can find applications in sorption of CO_2*, luminescence or catalysis.*

Keywords
Metal-organic frameworks, bimetallic, post-functionalization, green chemistry, mechanochemistry

1. Introduction

Highly porous materials, such as zeolites and activated carbons, are nowadays vital in many applications and industrial processes, including catalysis and gas storage. Among these porous materials with high surface area, metal-organic frameworks (MOFs), composed of metal nodes connected by organic bridging ligands, are a relatively new type of compounds that possess an unprecedented tunability [1-5]. Indeed, they can be composed of virtually any type of metal, or cluster, and organic linker molecules, which assemble to form porous architectures with a myriad of possible structures (Figure 1). MOFs can be mono or heterometallic, can possess more than one type of organic linkers with or without accessible functionalities, and can thus be designed specifically for a given purpose. Their porosity and tunable cages allow them to interact with guest molecules, taking advantage of both coordination chemistry on the metal sites and the availability of organic functions such as amines on the ligands [6]. Furthermore, the architecture of MOFs enables unprecedented properties, such as the possibility to create coordination vacancies through solvent removal in a rigid environment, leading to the creation of frustrated coordinated unsaturated sites (CUS) (Figure 2).

Among the wide variety of MOFs, our work focussed on three different structures with the possibility of creating such unsaturated sites based on a commercially available linker,

https://doi.org/10.52809/cn2022/VTMP8429

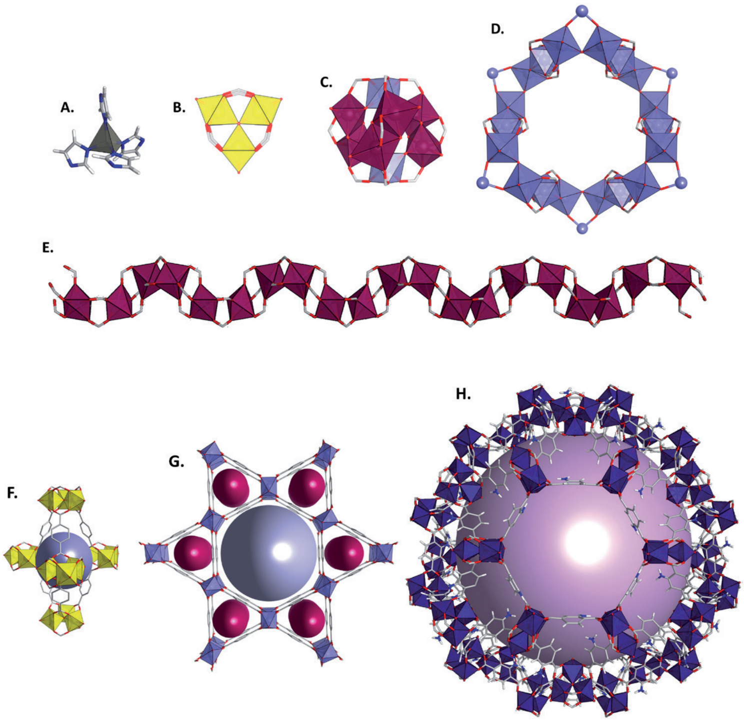

Figure 1. Example of the wide variety of building blocks (A. to E.) and porous structures (F. to H.) of MOFs. Linkers are represented by sticks (C = grey, O = red, N = blue and H = white), metal centres by polyhedra and pores by large spheres. (A.) Zn^{II} metal centre surrounded by 2-methylimidazolate linkers composing the ZIF-8 MOF, (B.) trinuclear M_3-μ_3-O cluster composing the series of isostructural MIL-100 MOFs (M = Al, Fe, Cr, V, etc.), (C.) Al octamers found in MIL-110(Al), (D.) hexagonal 18-membered rings found in MIL-96 and (E.) infinite chains composing the series of isostructural lanthanide-based MOF-76(Ln). The variety of pores are exemplified by the cages of (F.) MOF-235, (G.) the two types of infinite channels found in MIL-68 and (H.) the large mesopore of MIL-101-NH_2.

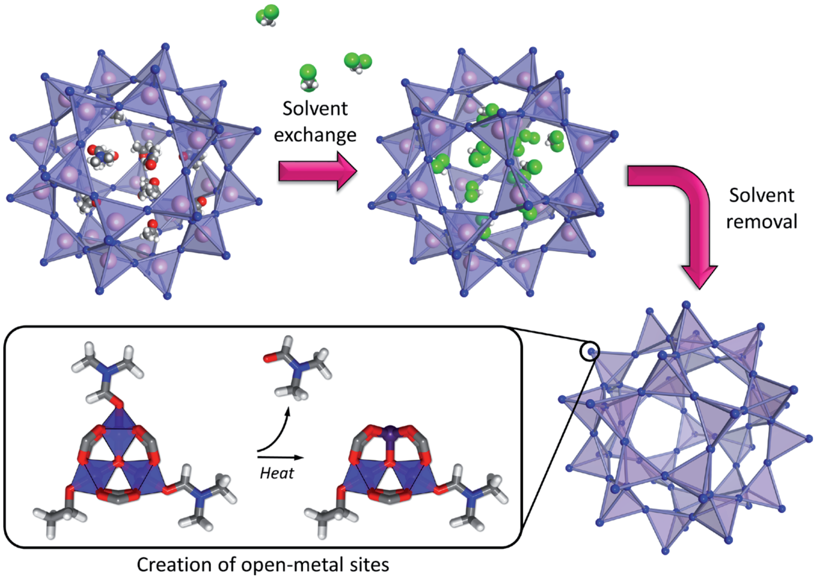

Figure 2. Illustration of the activation process of MOFs (illustrated by the example of MIL-101(Ti^{III})-NH_2), showing exchange of a coordinating solvent (*N,N*-dimethylformamide) by a more volatile one (dichloromethane) and removal of the solvent occupying the pores. The inset shows the removal of one coordinated solvent molecule (*N,N*-dimethylformamide) to lead to the formation of a coordinated unsaturated site. For the sake of simplicity, the large supertetrahedra composing the MOF, similar to the ones in MIL-100 (see further), are represented by tetrahedra from which the edges represent the 2-aminoterephthalate linkers and the blue spheres at the corners represent the cluster units where metal ions are situated (pink spheres represent micropores).

benzene-1,3,5-tricarboxylate (BTC^{3-}), also known as trimesic acid (Figure 3). Although those frameworks have a common rigid organic building brick, their structure is very different due to different connectivity topology. The commonly used pathways developed for synthesising them are usually based on approaches that are not compatible with the rules of green chemistry, implying the use of toxic, non-renewable and sometimes dangerous chemicals, and using significant amounts of energy to carry on the reactions, mostly under solvothermal conditions [7]. Hence, our goal is to find softer and less toxic synthesis methods and study the impact of these alternative pathways on those MOF structures.

Figure 3. Structure of the trimesate linker (C = grey, O = red and H = white).

2. Results

2.1. Green synthesis and metal-site functionalization of iron-based mono and bimetallic MIL-100 MOFs

MIL-100 is a class of MOFs composed of trinuclear μ_3-oxo centred metal clusters interconnected by six carboxylate functions, with solvent molecules completing the coordination spheres of each metal centre, and anions ensuring the clusters charge neutrality (see Figure 4, A. and B.). Four of those clusters are interconnected by four trimesate linkers to form supertetrahedra having the linkers as faces and the trinuclear clusters as vertexes (Figure 4, C.). Those supertetrahedra are further interconnected to yield a complex structure with two types of mesopores (Figure 4, D.). Interestingly, the solvent molecules on the metal sites can partly be removed by heating the frameworks under vacuum, leading to frustrated coordinatively unsaturated sites, also called “open-metal” sites. Those open-metal sites, whose amount in the structure mainly depends on the type of metal composing the MOF (mainly the case for Cr, Fe, V, Mn, Sc, Ti or combinations of several transition metals), are interesting as they have the ability to bind to various functions on target molecules. The binding efficiency mainly depends on the nature of the metal and its Lewis acidity and can thus be tuned, enabling applications in sorption or catalysis, among others.

Prior to the work described herein, the synthesis of MIL-100 MOFs was mainly performed under rather harsh and energy-demanding solvothermal conditions, starting from trimesic acid, and often using modulators that can present a danger to the operator, especially when used in large amounts (i.e. HNO_3, HF). In order to improve first the synthesis of the iron-based MIL-100(Fe), we developed a new green aqueous strategy through the use of alkali trimesate salts, which were all thoroughly characterized and whose structures have been solved by X-ray diffraction. The synthesis could easily be performed by stirring aqueous solutions of these linker salts and iron(II) sulfate, or any other water-soluble Fe(II) salt, in one step in the presence of air, independently of the nature of the alkali ion present in the precursor salt, within a reaction time of 3 hours (Figure 5) [8]. The MOF’s formation mechanism has been investigated and a Fe_3BTC_2 (BTC^{3-} = benzene-1,3,5-tricarboxylate) intermediate was isolated in the form of single crystals by performing the reaction under argon, allowing to elucidate its structure (see middle of Figure 5). It was shown that both water as solvent, and oxygen as oxidant are necessary for the transformation of this precursor into the target MOF, as other tested solvents and oxidants led to non-porous materials having a completely different crystal structure. Total or partial substitution of sodium trimesate by sodium 2-aminotrimesate during the synthesis allowed to obtain MIL-100(Fe) samples bearing amine functions on their linkers, although the MOF formation kinetics were slowed down by the introduction of the $-NH_2$ function on the linker.

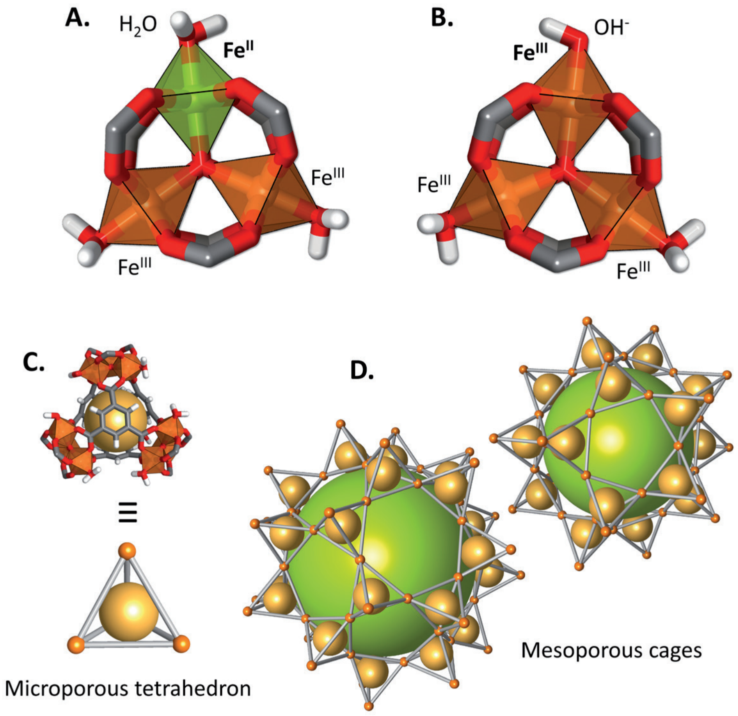

Figure 4. Structure of MIL-100 MOFs: (A. and B.) two possible structures of the clusters with Fe as metal (Fe^{III} = orange tetrahedra, Fe^{II} = green tetrahedra, C = grey, O = red and H = white), (C.) assembly of clusters by trimesate linkers to form supertetrahedra and (D.) the two types of mesopores formed by their interconnection.

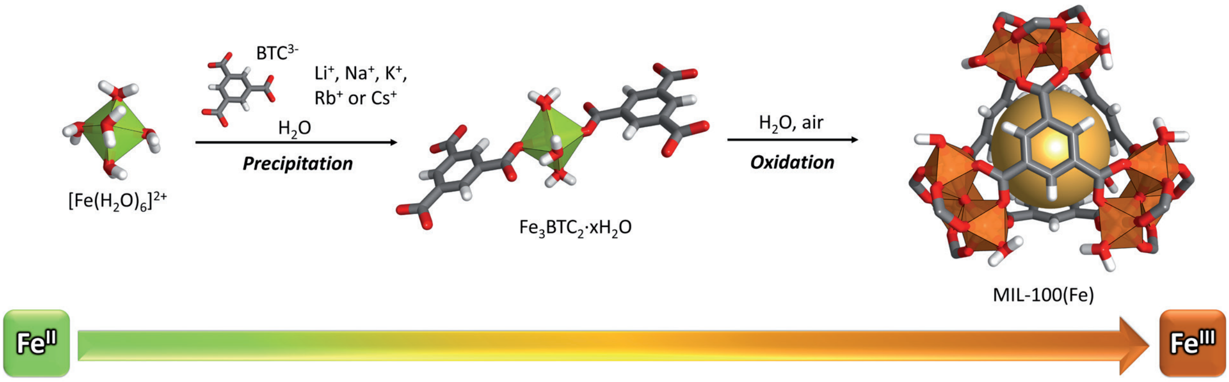

Figure 5. Reaction of Fe^{2+} with alkali trimesate salts in water to yield MIL-100(Fe) upon oxidation to Fe^{3+} in the presence of water and air, along with the structure of the isolated Fe^{II} intermediate (middle of the figure).

This new synthetic strategy was further developed to allow the incorporation of a second metal [9]. Bimetallic MIL-100(Fe,M) MOFs were successfully obtained with a plethora of transition, ρ-bloc and rare-earth elements as secondary metals in a one-pot fashion (M = Al, Ti, V, Cr, Mn, Co, Ni, Cu, Zn, Cd, La, Ce, Pr, Sm, Eu and Tb). The amount of incorporated doping metal, which could reach up to 20% of the total metal content without affecting the structure, could be controlled and it was demonstrated that metals in the +III oxidation state were incorporated preferentially into the framework over iron, that was in turn preferentially incorporated over metals in the +II oxidation state [9]. The use of the alkali salt as precursors enables the pH of the reaction medium to remain slightly acidic during the process, which was demonstrated to be crucial for the formation of the target MIL-100(Fe,M) MOFs as only crystalline phase in the obtained solids [9]. Such bimetallic MIL-100(Fe,M) derivatives can find uses in catalysis for example [10]. The obtained materials were also evaluated for their use in heat management through the reversible sorption of water and associated heat exchange processes (exothermic adsorption and endothermic desorption) with collaborators in Japan [11].

Upon the successful synthesis of MIL-100(Fe,M) MOFs through this new approach, the functionalization of mono- and bimetallic Al- and Fe-based MIL-100 MOFs with ethylenediamine (EN) was investigated [12]. This was performed with the idea of using one of EN's amine functions as anchor site to the CUS in the MOF, leaving the other, free, amine site exposed into the cavities of the framework for enabling interaction with guest molecules such as CO_2 or for further post-functionalization purposes exploiting the rich chemistry of amines (Figure 6, A.). It was shown that only Al-containing MOFs (both mono and bimetallic) could withstand contact with EN in toluene, whereas monometallic MIL-100(Fe) transformed into an amorphous and non-porous compound in the same conditions. Upon functionalization with ethylenediamine, MIL-100(Al), obtained with hierarchized porosity through a new solvothermal synthetic approach, [1,8] showed improved affinity for CO_2 in the low pressure range. Quantitative liquid-state ^{1}H-NMR on the digested MOF, as well as solid-state ^{13}C, ^{27}Al and natural abundance ^{15}N MAS-NMR allowed us to determine the local cluster structure of the functionalized MOF, composed of $Al_3\mu_3O$ (μ_3 stands for the triple bridging mode of the central O^{2-} ligand) units surrounded by one OH^- charge balancing anion, one water molecule, and one ethylenediamine molecule with one coordinated moiety and one free $–NH_2$ function (Figure 6, A.). Furthermore, this EN@MIL-100(Al) material contains both Brønsted acidic (Al) and basic ($-NH_2$) functions, as shown by the UV-visible spectra upon adsorption of bromothymol blue. The free amines of the functionalized MOF could be efficiently post-

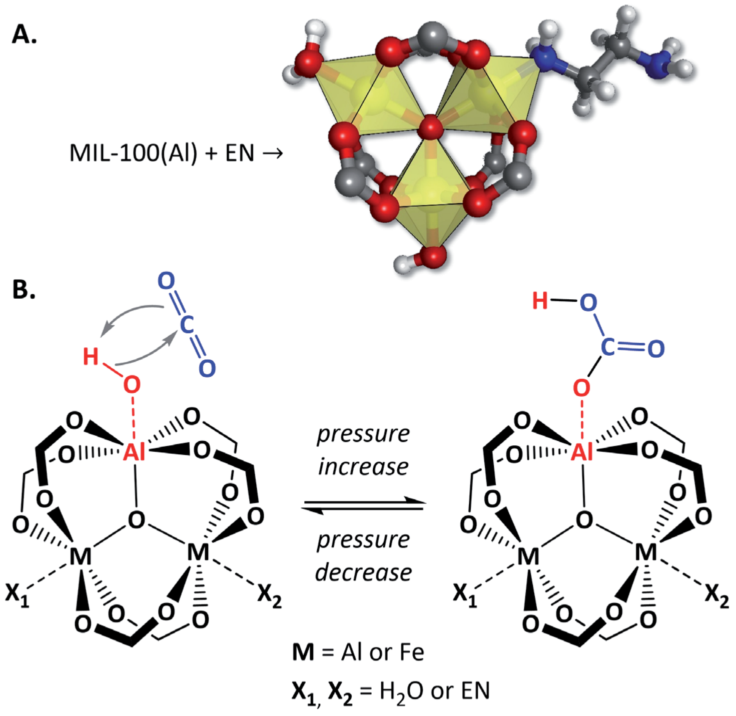

Figure 6. (A.) General scheme of the reaction of MIL-100 MOFs with ethylenediamine (EN) and the determined local structure of functionalized clusters in EN@MIL-100(Al) (Colour code: Al = yellow, O = red, C = grey, N = blue and H = white), and (B.) hypothesized reaction of the clusters of Al-containing MIL-100 MOFs with CO_2 under pressure.

functionalized by a fluorescent BODIPY probe and the functions inside the large mesoporous cages of the MOF could specifically react with ninhydrin thanks to size selectivity of the pore windows, further demonstrating the availability of the free $-NH_2$ functions. Al-containing MOFs, including the bimetallic MIL-100(Fe,Al), also showed an unexpected increase in CO_2 sorption at high pressures, above 20 bar. This behaviour makes the sorption isotherm incompatible with the simple Langmuir model, as the sudden increase of uptake deviates the curve from the ideal shape expected from this model. This is likely due to insertion of CO_2 in the AlOH bonds to form carbonic acid species that are not stable at lower pressures (Figure 6, B.).

2.2. Synthesis of MOF-76 in ethanol and linker functionalization

More sustainable strategies towards the synthesis of MOFs were further investigated for the rare-earth based isostructural family known as MOF-76. Those MOFs are composed of infinite chains of rare earth metals that are interconnected through trimesate linkers to form porous channels that can host guest molecules (Figure 7, A. and B.). Upon heating under vacuum and solvent de-coordination, the rare-earth metals centres are 6-coordinated to neighbouring oxygen atoms from the linker's carboxylates groups. This leads to the presence of one or more open-metal centres on the metal sites, as rare earths commonly have 7 to 9 available coordination sites depending on their size (Figure 7, C. and D.).

Through our new approach, based on reaction of soluble rare earth chlorides and trimesic acid in ethanol, those MOFs could be obtained at temperatures as low as room temperature, in the absence of the commonly used dimethylformamide (DMF), according to the following equation:

$$LnCl_3 + H_3BTC \rightarrow LnBTC\ (MOF\text{-}76) + 3\ HCl$$

This is of importance since DMF is often regarded as a non-desirable solvent due to its toxicity, tendency to coordinate strongly and its high boiling point. We evidenced an effect of

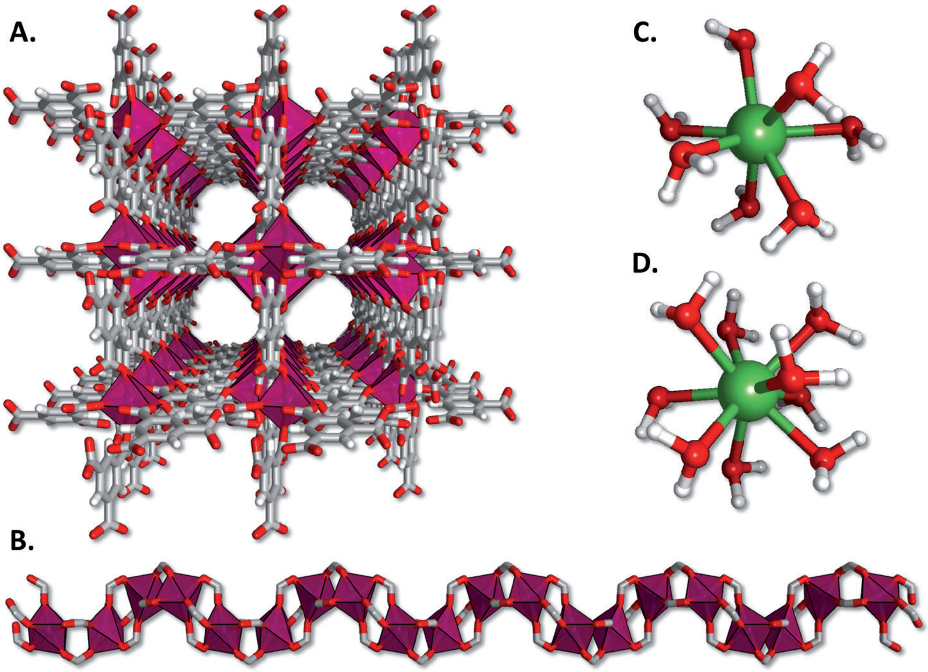

Figure 7. (A.) Structure of MOF-76 evidencing the porous channels and (B.) infinite chain building block, together with $[Ln(H_2O)_7]^{3+}$ and $[Ln(H_2O)_9]^{3+}$ ions, illustrating the diversity of coordination around Ln atoms. Colour code: Ln = purple polyhedra (A. and B.) and green atoms (C. and D.), C = grey, O = red and H = white.

the diameter of the rare-earth metal on the size of the obtained crystallites, as well as on the possibility to perform the synthesis, which only succeeded for the larger and smaller explored lanthanides (Ce, Pr, Nd and Yb), and lanthanum, but not for the intermediate ones (Sm, Eu, Tb and Er) (Figure 8). However, incorporation of medium sized lanthanides such as Eu or Tb in small amounts (typically 5%) during the synthesis enables to obtain bimetallic MOF-76 frameworks with luminescent properties. The synthesis mechanism has also been unravelled for MOF-76(La), through *in situ* and *ex-situ* and ^{1}H, ^{2}H, ^{13}C and ^{139}La solution-state NMR and pH measurements, showing that partial esterification of the linker is the reason why quite low yields were obtained, although the unreacted materials can be recycled. Interestingly, we evidenced an effect of the size of the rare-earth metal on the water stability of this MOFs series, which increases with decreasing radius of the metal. Indeed, the crystal structure of the La, Ce, Pr and Nd MOFs collapses upon a relatively short exposure to water or even humid air, whereas MOF-76(Yb) and MOF-76(Er) maintained their structure during prolonged soaking in water at 100°C (Figure 8). This is likely related to the presence of only one CUS on the smaller lanthanides (Er and Yb) compared to the larger rare earths.

The water stability could also be increased by substitution of the trimesate linker by 2-aminotrimesate, leading to a water stable MOF even with large La as metal centre. In addition, adding an amine function on the linker enables tuning the fluorescent properties of the frameworks, giving blue fluorescence for MOF-76(La)-NH_2 (Figure 9, inset), an important enhancement of the quantum yield of the green luminescent MOF-76(Tb)-NH_2 and quenching of the luminescence of the MOF-76(Eu)-NH_2. Xenon adsorption in MOF-76(La) was also investigated by *in situ* PXRD, revealing an interesting structural transformation (Figure 9, A. and B.). This might lead to applications of this MOF for xenon storage, which is a useful gas in lighting and medical fields.

2.3. Mechanochemical synthesis of HKUST-1 and characterization of defect sites

Finally, the introduction of structural defects into mechanochemically obtained HKUST-1, a framework regarded as a model MOF, based on Cu-Cu paddlewheel units linked by trimesates (Figure 10, left), was investigated [13]. Samples were obtained by salt-assisted (SAG, with NaCl) mechanochemical methods and different post-synthetic treatments, consisting of washing with either ethanol or methanol, and drying at

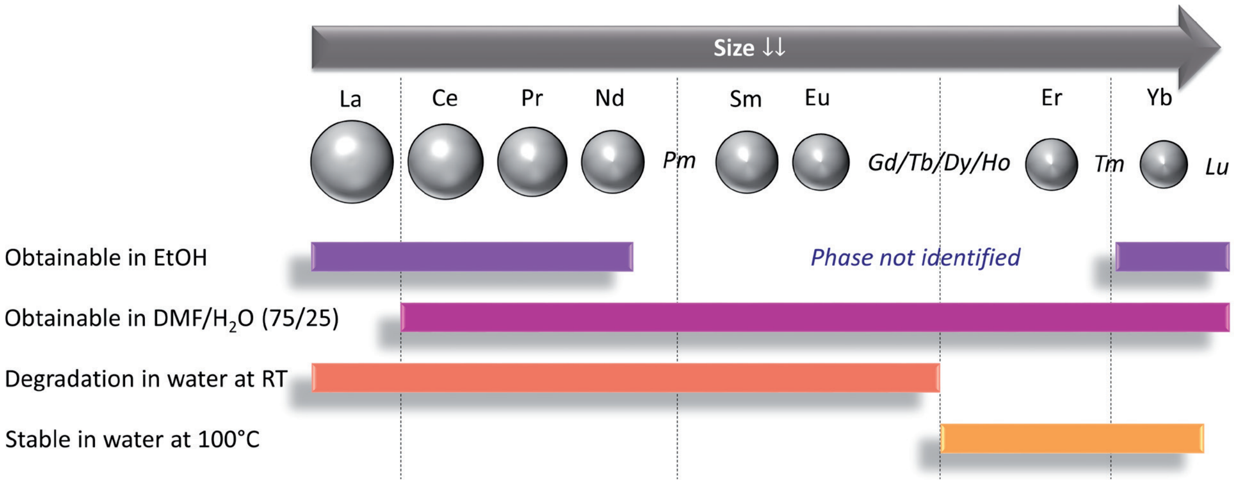

Figure 8. Scheme of synthesis and stability conditions of MOF-76, in function of the used lanthanide (the tested lanthanides are represented by the grey spheres; intermediate elements that were not tested are indicated by the chemical symbols only). For information, the ionic radii of La^{3+} and Yb^{3+} are 1.032 Å and 0.868 Å, respectively.

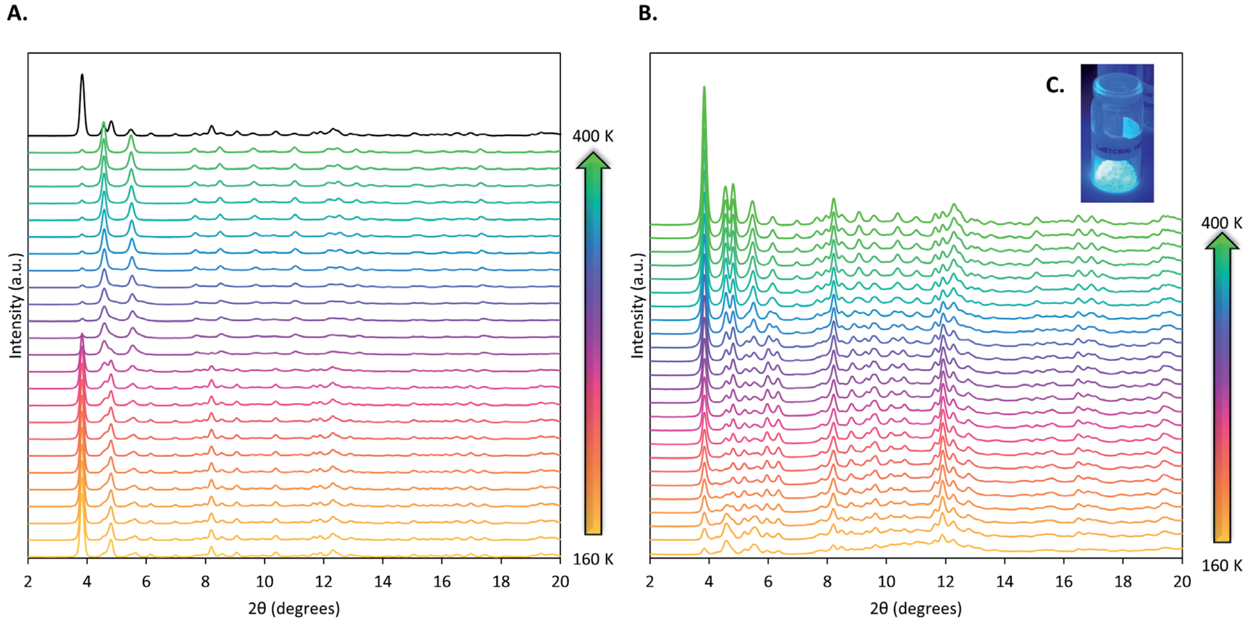

Figure 9. Variable temperature PXRD patterns of MOF-76(La) (A.) under vacuum and (B.) under 1.10 bar of xenon. The black pattern represents the sample after overnight heating under vacuum at 400 K. The blue fluorescence of MOF-76(La)-NH_2 under UV irradiation is shown in the inset (C.).

different temperatures (Figure 10, right). This procedure leads to acetic acid as the only by-product and drastically reduces the amount of solvent required for the synthesis, which is performed at room temperature and can thus be regarded as a green approach.

It was shown by combination of multiple characterization methods that treatment with

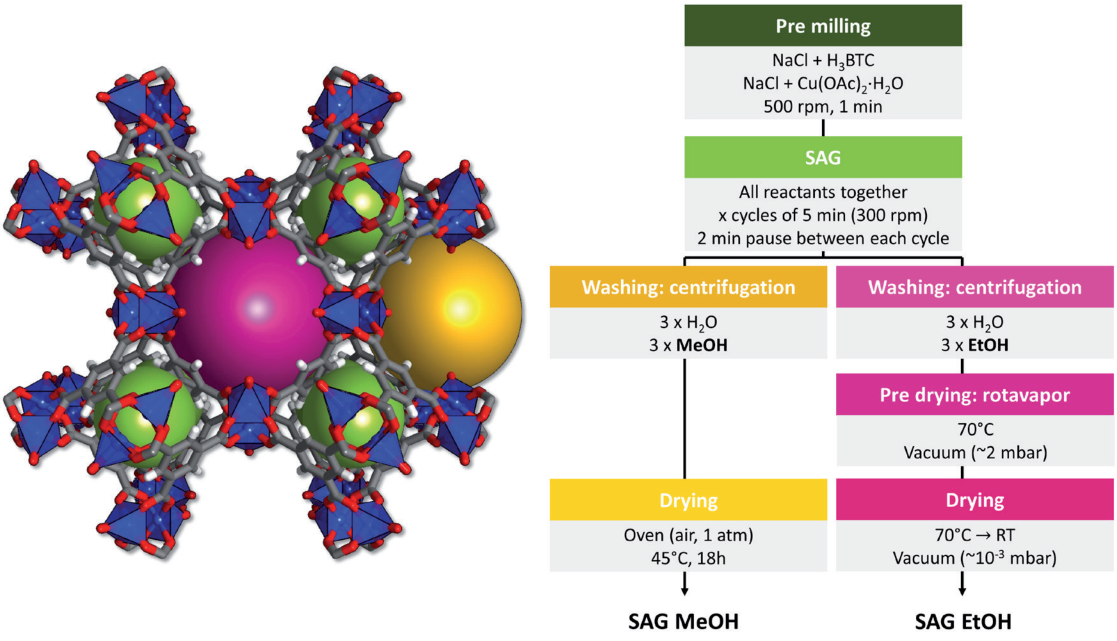

Figure 10. Structure of HKUST1 (left) and synthesis conditions for samples obtained by SAG (right). Colour code: Cu = blue polyhedra, C = grey, O = red and H = white. Coloured spheres represent the pores.

methanol induces the creation of copper(I) (Cu^I) defects, evidenced by X-ray photoelectron spectroscopy (XPS), whereas treatment with ethanol creates defects in the form of free –COOH functions, as evidenced by IR spectroscopy (Figure 11). The amount of those defects was dependent on the grinding time of the mechanochemical procedure, which also had an influence on the textural properties. Surprisingly, when the samples were treated with methanol, the surface area increased with increasing grinding time, whereas treatment with ethanol led to a more classical decrease in surface area with increasing grinding time. This result could indicate that the treatment with ethanol has a "healing" effect on the defects in the MOF structure. Synthesis of HKUST-1 using liquid-assisted grinding with a bit of ethanol, instead of dry NaCl-assisted grinding, resulted in a MOF with a very low amount of structural defects, even when compared to single crystals obtained by a more classical but less green solvothermal approach, resulting in a MOF containing a low amount of Cu^I-type defects.

Concerning the structure-properties relationship of the obtained HKUST-1 MOFs, it was shown that carboxylic acid defects have a negative impact on both CO_2 sorption and catalytic cyclopropanation activity, i.e. decreasing CO_2 uptakes in the first case and no conversion of styrene and ethyldiazoacetate into cyclopropanes in the second case, respectively (Table 1). Interestingly, the presence of Cu^I defects was able to partly counteract the poisoning effect in catalysis. Indeed, in the presence of carboxylic acid defects, the co-existence of Cu^I-type defects led to some conversion of styrene into the desired product. Finally, HKUST-1 obtained from liquid-assisted grinding and which has nearly no defects, seems to be the best material for catalytic cyclopropanation, whereas the solvothermally obtained large crystals with small amounts of Cu^I defects showed the highest CO_2 gravimetric uptake. These results show how different types of defects can be introduced into MOFs by mechanochemical synthesis, also giving a hierarchical porosity. Those defects and modulated porosity were shown to have an impact on the performances towards applications.

3. Conclusion

Although MOFs are becoming more and more popular, and despite industrial applications are emerging timidly, control on the synthesis of those materials remains challenging. The work presented in here mainly aims at improving the sustainable production of MOFs based on trimesate linkers, with well-characterized structures, as well as at the introduction of new types of active sites, under the form of second ("exotic") metals, amine functions and defects, by easy-to-implement synthetic approaches. Those materials may find use in multiple applications, such as, but not limited to, catalysis and gas sorption.

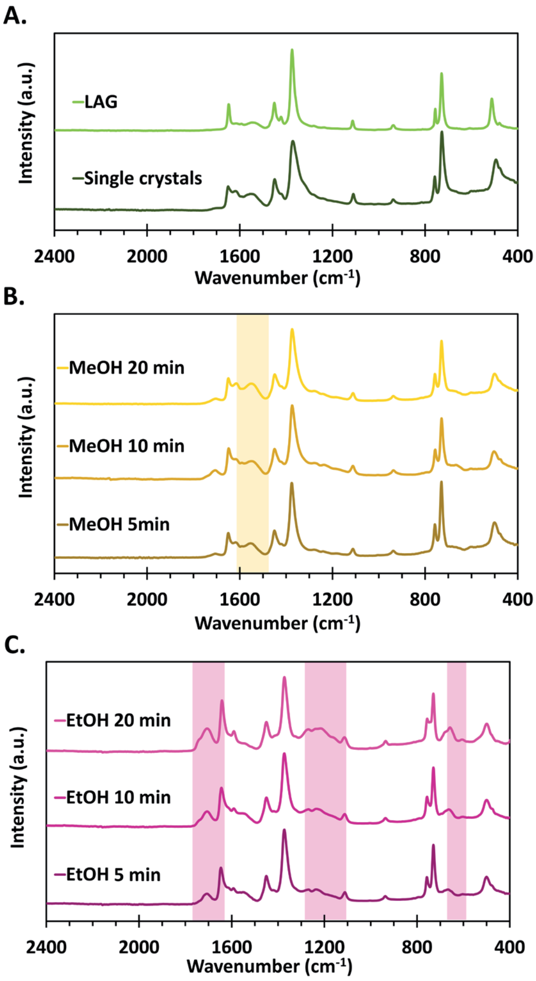

Figure 11. Attenuated total reflectance FTIR spectra of HKUST-1 samples obtained by (A.) liquid-assisted and as single crystals from conventional solvothermal synthesis or by SAG with different milling times followed by a treatment with (B.) MeOH or (C.) EtOH.

Sample	Conversion of ethyldiazoacetate (%)	Selectivity (%)		CO_2 uptake at first adsorption (wt. %)
		Cis-cyclopropane	*Trans*-cyclopropane	
Single crystals	93	13	31	17
Liquid-assisted grinding (LAG)	100	20	43	11
SAG 5 min MeOH	7	6	15	11
SAG 10 min MeOH	15	13	19	7
SAG 20 min MeOH	100	13	21	7
SAG 5 min EtOH	2	–	–	5
SAG 10 min EtOH	0	–	–	5
SAG 20 min EtOH	0	–	–	4

Table 1. Results of catalytic cyclopropanation of ethyldiazoacetate with styrene and CO_2 uptake using the different HKUST-1 samples as catalysts.

References

[1] T. Steenhaut, Y. Filinchuk, S. Hermans, *Journal of Materials Chemistry A* **2021**, *9* , 21483.

[2] S. Liu, Y. Qiu, Y. Liu, W. Zhang, Z. Dai, D. Srivastava, A. Kumar, Y. Pan, J. Liu, *New Journal of Chemistry* **2022**, *46*, 13818.

[3] N. Stock, S. Biswas, *Chemical Reviews* **2012**, *112*, 933.

[4] S. Dai, A. Tissot, C. Serre, *Bulletin of the Chemical Society of Japan* **2022**, *94*, 2623.

[5] G. Mouchaham, F. S. Cui, F. Nouar, V. Pimenta, J.-S. Chang, C. Serre, *Trends in Chemistry* **2020**, *2*, 990.

[6] M. Benzaqui, M. Wahiduzzaman, H. Zhao, M. R. Hasan, T. Steenhaut, A. Saad, J. Marrot, P. Normand, J.-M. Grenèche, N. Heymans, G. De Weireld, A. Tissot, W. Shepard, Y. Filinchuk, S. Hermans, F. Carn, M. Manlankowska, C. Téllez, J. Coronas, G. Maurin, N. Steunou, C. Serre, *Journal of Materials Chemistry A* **2022**, *10*, 8535.

[7] T. Steenhaut, S. Lacour, G. Barozzino-Consiglio, K. Robeyns, R. Crits, S. Hermans, Y. Filinchuk, *Inorganic Chemistry* **2022**, *61*, 11084.

[8] T. Steenhaut, ‘Synthesis strategies towards new heterometallic and functionalized MOFs’, PhD dissertation, Université catholique de Louvain, http://hdl.handle.net/2078.1/263445, **2022**.

[9] T. Steenhaut, S. Hermans, Y. Filinchuk, *New Journal of Chemistry* **2020**, *44*, 3847.

[10] R. Crits, ‘Study of the influence of the nature of metals, anions, and linker functionalities on the stability of Metal-Organic-Frameworks (MOFs) with the MTN topology’, Master thesis dissertation, Université catholique de Louvain, http://hdl.handle.net/2078.1/thesis:37560, **2022**.

[11] T. H. Rupam, T. Steenhaut, M. L. Palash, Y. Filinchuk, S. Hermans, B. B. Saha, *Chemical Engineering Journal* **2022**, *448*, 137590.

[12] T. Steenhaut, L. Fusaro, K. Robeyns, S. Lacour, X. Li, J. G. Mahy, V. Louppe, N. Grégoire, G. Barozzino-Consiglio, J.-F. Statsyns, C. Aprile, Y. Filinchuk, S. Hermans, *Inorganic Chemistry* **2021**, *60*, 16666.

[13] T. Steenhaut, N. Grégoire, G. Barozzino-Consiglio, Y. Filinchuk, S. Hermans, *RSC Advances* **2020**, *10*, 19822.